Contents list available at CBIORE journal website

International Journal of Renewable Energy Development

Journal homepage: https://ijred.cbiore.id

Research Article

Numerical simulation of a novel small water turbine generator for installation in a deep-flow hydroponics system

Werayoot Lahamornchaiyakul*

Department of Mechanical Engineering, Rajamangala University of Technology Lanna Phitsanulok, Phitsanulok 65000, Thailand

Abstract. Hydroponics systems are crucial for providing sustainable and cost-effective choices when soils are unavailable for conventional farming. The application of water flow rates within hydroponics systems to generate electricity is another idea that can be used in the field of power generation. This paper presents the determination of the mechanical power efficiency of a novel small water turbine generator for use in a deep-flow hydroponics system (DFT). The system was designed, analysed, and calculated for the most suitable geometries of the water pipeline inlet, DFT system, main structure of the PVC Tee Pipe Fitting, and a water turbine wheel using computational fluid dynamics software. The diameter of the water turbine wheel in this research was 48 mm. A DFT hydroponic system was modelled for the purposes of this research. We conducted a numerical simulation with water flow rates of 6, 8, and 10 l/min to evaluate the turbulent kinetic energy distribution in the DFT hydroponic system. The numerical simulation employed the control volume methodology, and the k-epsilon turbulence model was applied to obtain the computational conclusions. The highest torque and power that a novel small water turbine for installation in a DFT system could generate at a maximum flow rate of 0.000167 m^3/s were 0.082 N.m. and 1.9568 watts, respectively. The forces generated by the fluid's speed and pressure can then be transferred to the building process of a novel small water turbine wheel. The FEA numerical result shows that the maximum value of the total deformation at a wheel speed of 228 rpm is 7.0 x 10^{-5} mm. The numerical simulations used in this study could potentially be used to further develop prototypes for innovative miniature water turbines that generate commercial electricity.

Keywords: computational fluid dynamics, 3d design, water turbine generator, deep flow technique, hydroponics

Received: 25th August 2023; Revised: 5th Oct 2023; Accepted: 26th Nov 2023; Available online: 6th Dec 2023

1. Introduction

Hydroponics is considered of great importance to Thailand's urban communities (Phaengkieo *et al.,* 2019). Due to urbanization and the need to accommodate workers coming to Thailand to participate in various businesses, the urban population has increased. Therefore, modern utilities must be provided to support the population, such as electric trains, buses, and, most importantly, housing in the form of detached houses, apartments, and commercial buildings.

Consequently, land in large cities has become very expensive, and there is less usable space for the construction of detached houses, and the range of house prices needs to be appropriate for the current economic conditions and afford able for salaried employees. In addition, various projects in residential areas tend to have limited space for plants and trees. For this reason, hydroponic soil-free cultivation plays a very important role nowadays because less space is required for cultivation, and no time is wasted in preparing the soil (Phaengkieo *et al.,* 2019; Jaruwongwittaya *et al.,* 2015). Hydroponic, soil-free cultivation not only allows various crops in limited space, but business groups have adopted the technique to grow organic vegetables for both domestic consumers and export. As a result, the business has rapidly expanded from a medium to a large industry. There are many forms of hydroponic cultivation, such as the Nutrient Film Technique (NFT), Deep-Flow Technique (DFT), and Dynamic Root Floating Technique (DRFT), each with its own functional characteristics (Phaengkieo *et al.,* 2019; Guzman-Valdivia *et al.,* 2019; Niam *et al.,* 2017; Vega *et al.*, 2023). In particular, DFT is commonly used by small and medium-sized businesses (SMEs) to grow vegetables in Thailand since PVC pipes are used as troughs to move water mixed with nutrient-dissolving lines and are cost-effective to build.

However, the limitation of hydroponic cultivation using DFT is that it requires electricity to operate the pump, driving the nutrient solution to the roots 24 hours a day (Kumkuang 2017; Baiyin *et al.*, 2021). Many previous works have studied the application of hydroponic techniques to produce soilless crops, such as those conducted at flow rates of 8 liters per minute and 10 liters per minute (Phaengkieo *et al.,* 2019; Kumkuang 2017; Baiyin *et al.,* 2021). Recently, Lahamornchaiyakul and Kasayapanand (2023) studied the generation of electricity from drainage lines and produced electricity from the flow inside the pipeline with a vertical-axis water turbine by analyzing the flow field to calculate the torque and electrical power using computational fluid dynamics techniques. In addition, various researchers have studied the production of electrical power from the flow of water inside pipes from water turbines in various forms. (e.g., Chen *et al.,* 2021; Chen *et al.*, 2013; Hasanzadeh *et al.*, 2021; Hosain *et al.,* 2020; Jiyun *et al.*, 2020; Ma *et al.,* 2020; Gandhi *et al.,* 2019 Muhammad *et al.,* 2020).

* Corresponding author
Email: werayootrmutl@gmail.com (W. Lahamornchaiyakul)

https://doi.org/10.14710/ijred.2024.58247
ISSN: 2252-4940/© 2024.The Author(s). Published by CBIORE

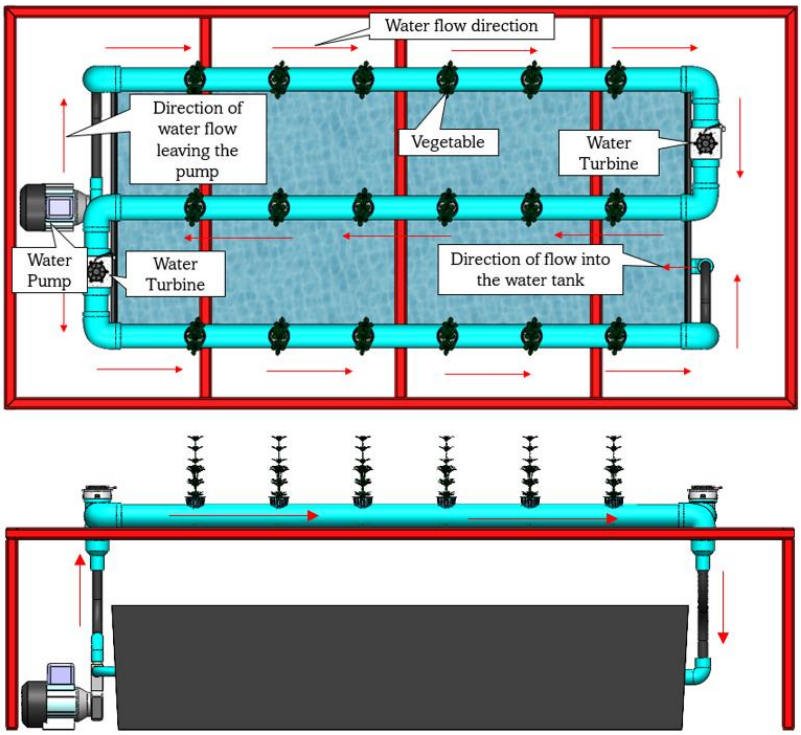

Fig. 1 A set of equipment and the direction of water inside the vegetable hydroponic pipeline

Nowadays, computational fluid dynamics (CFD) is popularly used to calculate the performance of various types of water turbines (Abdulah and Muhammed, 2022; Lahamornchaiyakul and Kasayapanand, 2023; Zhuohuan *et al*., 2020; Yeo *et al*., 2019) and pump designs (Wang *et al*., 2022). Thermal analysis in the design of the heat exchanger equipment (Dmitriev *et al.,* 2023), as well as air conditioner wind speed analysis (Patel and Dhakar, 2018). A car body that simulates airflow has also been designed (Thabet and Thabit, 2018).

The principles of the fluid inside the pipe and the design guidelines for small water turbines found in the abovementioned research originate from the design and analysis of a novel small water turbine generator for installation in a deep-flow hydroponics system using CFD. The present study demonstrates the performance of a novel small water turbine designed to be installed within a PVC pipe system used for growing hydroponic vegetables, including the steps required to analyze the fluid flow field at various positions within the designed PVC pipe. The findings can be used as a guideline for further research on the production of energy from the water circulating within hydroponic vegetable growing pipes in Thailand.

2. Model of Numerical Simulation

This research employs a circulating flow system with a pump to suck water from the reservoir on the front side to flow along the PVC pipe and back into the reservoir at the rear of the tank, as shown in Fig. 1.

Fig. 1 shows the flow rates used in past studies, ranging from 8 liters per minute to 10 liters per minute with sufficient water volume for power generation with small, vertical turbines used for the installation through a PVC pipeline. The turbine is installed through a PVC tee pipe assembly device. The design of a novel small water turbine in this research requires consideration of data in the form of the DC 12V Model GOSO F50-12V. A small generator, purchased from Shenzhen Global Technology and readily available on the market, is also employed, as shown in Fig. 2.

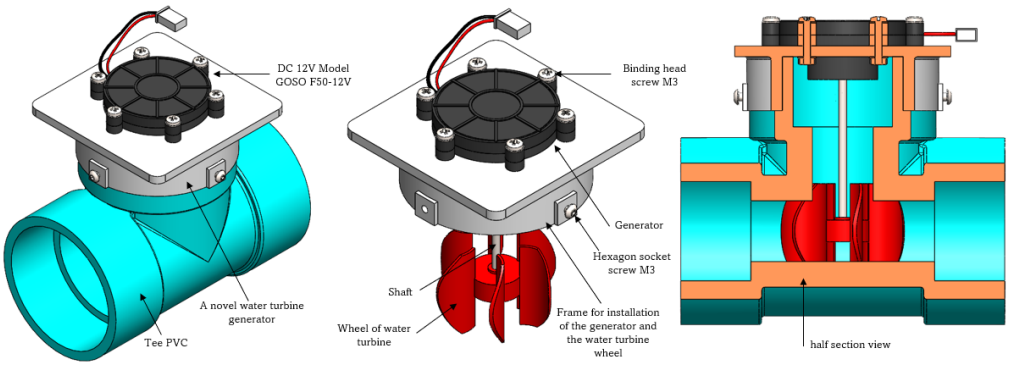

Fig. 2 A novel water turbine generator for installation in the vegetable hydroponic pipeline; (a) The model of a novel water turbine generator; (b) Detail of a novel water turbine generator and (c) Half-section view of a novel water turbine generator

2.1 CFD Model

The Navier-Stokes equation, based on continuum and momentum theory, is used to explain the incompressible flow pattern through turbomachinery. In this study, the CFD model of a novel small water turbine for installation in a deep-flow hydroponics system is shown in the form of Navier-Stokes equations, expressed by Equations 1–4 (Lahamornchaiyakul and Kasayapanand, 2023; Mosbahi *et al.*, 2019; McLean, 2012; Muhammad *et al.*, 2021; Muhammad *et al.*, 2020; Anas *et al.*, 2022; Wisatesajja *et al.*, 2021; Ghada *et al.*, 2022).

$$\frac{\partial \rho}{\partial t} + \frac{\partial (\rho u_i)}{\partial x_i} = 0 \quad (1)$$

$$\frac{\partial (\rho u_i)}{\partial t} + \frac{\partial}{\partial x_j}(\rho u_i u_i) + \frac{\partial P}{\partial x_i} = \frac{\partial}{\partial x_i}(\tau_{ij} + \tau_{ij}^R) + S_i \quad (2)$$

$$\frac{\partial \rho H}{\partial t} + \frac{\partial \rho u_i H}{\partial x_i} = \frac{\partial}{\partial x_i}(u_j(\tau_{ij} + \tau_{ij}^R) + q_i) + \frac{\partial p}{\partial t} - \tau_{ij}^R \frac{\partial u_i}{\partial x_j} + \rho\varepsilon + S_i u_i + Q_H \quad (3)$$

$$H = h + \frac{u^2}{2} \quad (4)$$

The SolidWorks Flow Simulation software consists of a system of key equations used to describe phenomena related to the flow of kinetic energy with turbulent flow (Patel *et al.*, 2016; Nasir, 2013 expressed as Equations 5– 8) (Sobachkin *et al.*, 2013; Hosain *et al.*, 2020; Lahamornchaiyakul and Kasayapanand, 2023).

$$\frac{\partial \rho k}{\partial t} + \frac{\partial \rho k u_i}{\partial x_i} = \frac{\partial}{\partial x_i}\left(\left(\mu + \frac{\mu_t}{\sigma_k}\right)\frac{\partial k}{\partial x_i}\right) + \tau_{ij}^R \frac{\partial u_i}{\partial x_j} - \rho\varepsilon + \mu_t P_B \quad (5)$$

$$\frac{\partial \rho \varepsilon}{\partial t} + \frac{\partial \rho \varepsilon u_i}{\partial x_i} = \frac{\partial}{\partial x_i}\left(\left(\mu + \frac{\mu_t}{\sigma_\varepsilon}\right)\frac{\partial \varepsilon}{\partial x_i}\right) + C_{\varepsilon 1}\frac{\varepsilon}{k}\left(f_1 \tau_{ij}^R \frac{\partial u}{\partial x_j} + C_B \mu_t P_B\right) - f_2 C_{s1}\frac{\rho\varepsilon^2}{k} \quad (6)$$

$$\tau_{ij} = \mu S_{ij}, \tau_{ij}^R = \mu_t S_{ij} - \frac{2}{3}\rho k \delta_{ij}, \quad S_{ij} = \frac{\partial u_i}{\partial x_j} + \frac{\partial u_j}{\partial x_i} - \frac{2}{3}\delta_{ij}\frac{\partial u_k}{\partial x_k} \quad (7)$$

$$P_B = -\frac{g_i}{\sigma_B}\frac{1}{\rho}\frac{\partial \rho}{\partial x_i} \quad (8)$$

where $C_\mu = 0.09, C_{\varepsilon 1} = 1.44, C_{\varepsilon 2} = 1.92, \sigma_k = 1,\ \sigma_\varepsilon = 1.3, \sigma_B = 0.9, C_B = 1\ if\ P_B > 0, C_B = 0$

if considering $P_B < 0$ so, the turbulence viscosity is determined from $\mu_t = \frac{C_\mu \rho k^2}{\varepsilon}$

2.2 FEA Model

In this case, Equation 9 determines the governing equation for the linear static finite element analysis (Lahamornchaiyakul, 2021; Lahamornchaiyakul, 2023; Lahamornchaiyakul and Kasayapanand, 2023; Vaishaly *et al.*, 2015). A finite element model is a structure made up of a node and an element. When only one node is considered, the degree of freedom has a maximum of six independent variables. Fig. 3 depicts the finite element model in this instance.

$$[K]\{q\} = \{F\} \quad (9)$$

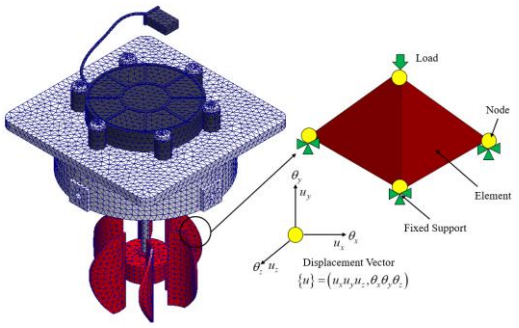

Fig. 3 Detail of the FEA mesh element in this research

where $[K]$ is Structural stiffness; $\{q\}$ is Nodal displacement, and $\{F\}$ is Load matrix Lahamornchaiyakul and Kasayapanand, 2023; Lahamornchaiyakul, 2023).

3. Water Turbine Design

3.1 CFD Model

The water flow rate is computed in this study by measuring the velocity of the water and the cross-section area of the pipeline for a water turbine installation using the deep-flow technique hydroponics system, as shown in Equation 10.

$$Q = Av \quad (m^3/s) \quad (10)$$

The water flow rates in this research for a novel small water turbine design are selected as Q = 6 l/min, 8 l/min, and 10 l/min, respectively.

3.2 Power of the Water Turbine

The power output of a novel small water turbine generator installed in the pipeline of a deep-flow hydroponics system is known as water turbine power. The power of a water turbine may be calculated using Equation 11.

$$P = \rho g Q H_n \quad (11)$$

In this research, approximately 80% efficiency is applied to the novel small water turbine generator for installation in a water pipeline for a deep-flow hydroponics system. The power output can be calculated according to the formula proposed by El-Sayed *et al.* (2019) and Lahamornchaiyal and Kasayapanand, (2023), as shown in Equation 12.

$$P = \eta \times \Delta P \times Q \quad (12)$$

Data:
1. Efficiency 80% (0.80).
2. Loss of pressure head (h_L) = 0.5 m.
3. Pipe diameter (D_P) = 50.8 mm (2 in)
4. Wheel water turbine diameter (D_o) = 48 mm.
5. Velocity = 0.082 m/s (10 l/min).

3.3 Water Turbine Speed (N)

Water turbine speed can be calculated from Equations 13, and 14 (Ebhota *et al.*, 2015; Abdulah *et al.*, 2022).

$$N = \frac{\omega \times 60}{2\pi} \quad (RPM) \quad (13)$$

$$\omega = \frac{V}{R} \quad (rad/s) \tag{14}$$

where N is the rotation speed (RPM), and ω is the omega velocity, while V is the water speed and R is the radius of the wheel turbine.

3.4 The blade spacing design (t_B)

In this research, Equation 15 may be used to calculate the tangential blade separation (Patel *et al.*, 2016; Nasir, 2013).

$$t_B = 0.174 \times D_o \quad (mm) \tag{15}$$

3.5 Number of runner blades (n)

The number of runner blades can be determined from Equation 16 (Patel *et al.*, 2016; Nasir, 2013).

$$n = \frac{\pi \times D_o}{t_B} \tag{16}$$

3.6 Blade radius curvature (r_B)

In this research, the blade radius curvature can be determined from Equation 17 (Patel *et al.*, 2016; Nasir, 2013).

$$r_B = 0.163 \times D_o \tag{17}$$

3.7 Shaft Diameter Design (D_s)

This study focuses on the optimal shaft diameter design for a novel small water turbine generator to support the highest water force produced on the water turbine shaft construction. The shaft diameter may be calculated using Equation 18 (Lahamornchaiyal and Kasayapanand, 2023).

$$D_s = 0.22 \times D_o \tag{18}$$

In this research, the equation system connection (12–18) is used to calculate and identify the proper percentage for the set of a novel water turbine wheel installed in a water pipeline of a DFT system. The size of the pipeline in this research is two inches, and the results are presented in Fig. 2.

3.8 Time step for CFD simulation (T_S)

In this research, the time step size for computational fluid dynamics may be calculated using equation (19) (Oladosu *et al.*, 2018; Autodesk Simulation CFD, 2022; Lahamornchaiyal and Kasayapanand, 2023).

$$T_s = \frac{D_o}{(N \times 6)} \tag{19}$$

4. Numerical Simulation Setting

4.1 CFD Simulation Setting

The water turbine analysis model in this research is designed to be installed on two-inch PVC pipes 1,500 millimeters in length, with three pipes connected to the pipe fittings (e.g., 90-degree elbows and PVC pipe tee fittings) at an installation distance of 330 mm. The PVC pipe is then drilled to install the plant pot with a planting distance of 215.50 mm, as shown in Fig. 4(b).

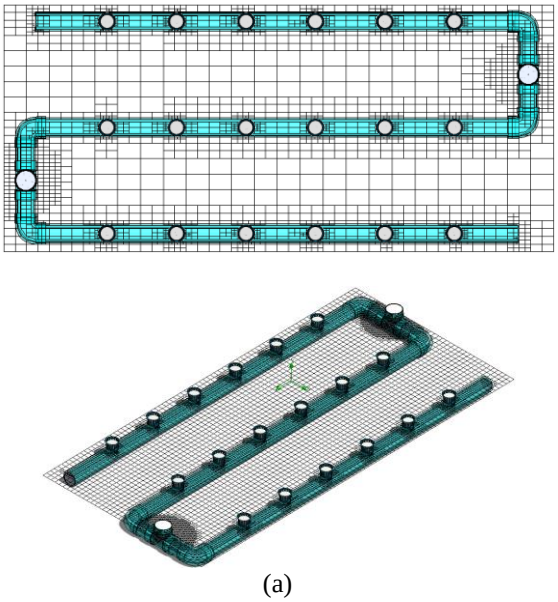

(a)

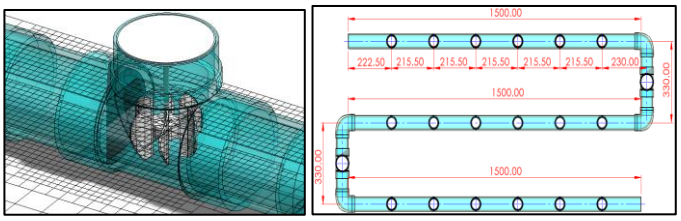

(b) (c)

Fig. 4 Illustration of CFD Mesh Structure of (a) The computational domain and (b) A novel small water turbine generator (c) Mesh properties in this research (c) Dimensions installation of a water pipeline of a deep flow technique system in this research

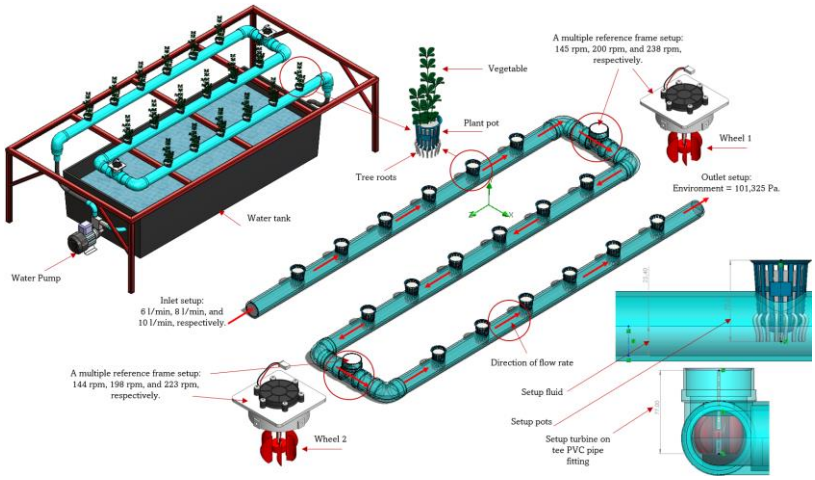

Fig. 5 Boundary condition in this research

Table 1
Specific properties of the mesh elements

Mesh type	Solid Mesh
Mesher used	Quadrilateral element
Total nods	79,200
Total element	215,131
Level of Refining Fluid Cell	2
Basic Mesh Dimensions	Nx = 40, Ny = 8, Nz = 84
Maximum Channels Refinement Level	2
Number of Cells Across Chanel	5

Source: (Solidwork Flow Simulation, 2022)

SolidWorks Flow Simulation is used for the CFD simulation, executed with a time step of 0.0135 seconds (Lahamornchaiyal and Kasayapanand, 2023), over a duration of 10 seconds. The entrance volume flow rate is imposed, with the environmental pressure at the output boundary at 101325 Pa (Lahamornchaiyal and Kasayapanand, 2023). The rotating area module is used to forecast the wheel rotation, which is set to 145, 200, and 238 RPM at volume flow rates of 6 L/min, 8 L/min, and 10 L/min, respectively.

The mesh elements of the various sections in this research are illustrated in Fig. 4, with the mesh sources in the tests investigated using a conventional k-epsilon turbulence model. Table 1 showed the generated meshing properties of the present model. The total number of elements generated is 350,000. Table 1 shows the specific properties of the mesh elements used to calculate the flow field and the electrical power generated by a novel small water turbine generator.

Fig. 4 shows the entire computational domain, subdivided into about 215,131 quadrilateral mesh elements. The CFD meshing part of SolidWorks Flow Simulation is employed to convert the continuous domain into a discrete section, with meshing validation performed starting with the third-level mesh under the option of the SolidWorks Flow Simulation software and progressing to the best mesh. Fig. 4 depicts the mesh components of the various parts. The meshing of each section is not uniform in terms of element size, as evident from Fig. 4. The variation is a result of the intricate nature of the curve on the water turbine wheel surface, necessitating the use of a novel and finely detailed element size for the small water turbine wheel. Fig. 5 depicts the boundary condition setup in this study.

In Fig. 5 of this research, a deflector device was considered for installation into a tee PVC pipe fitting to increase the speed

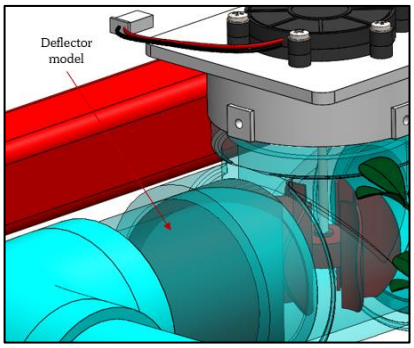

Fig. 6 Position of the deflector installation

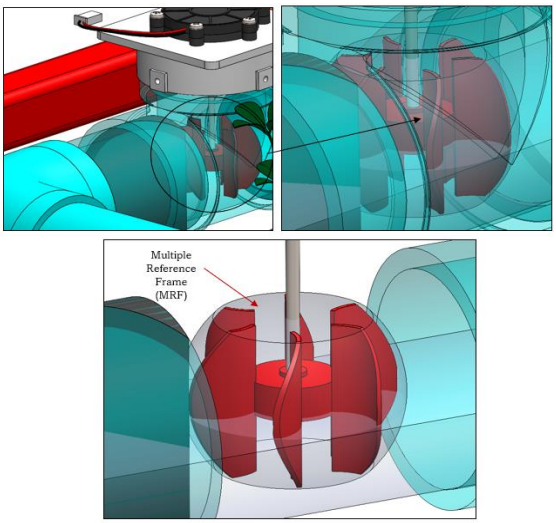

Fig. 7 Multiple reference frames (MRF) in this research

of the water stream before entering the water turbine wheel assembly. The deflector device is shown in Fig. 6. When the calculation results meet these criteria, it is assumed that the numerical calculations approach the answer according to the prerequisites. The rotation analysis region is initially modeled to determine the Multiple Reference Frame (MRF) together with the stationary target, which is defined as stationary. The mesh element, also known as an MRF is shown in Fig. 7.

Fluid flow around the rotating components or systems is simulated using an MRF. It examines the flow fields in turbines, pumps, and fans. The rotating area is divided into stationary reference frames for each rotating component using an MRF. The MRF approach simplifies the computing cost of flow field simulation in rotating component systems. It investigates flow separation, recirculation, and vortex shedding near rotating machinery. The aerospace, automotive, and energy sectors use the MRF to develop and optimize rotating systems (MR CFD Company, 2023).

The purpose of providing boundary conditions in CFD is to constrain the discrete form of the equation so that it may be solved in a specified framework while also illustrating the flow characteristics of the computational domain.

4.2 Assumptions on CFD Simulation

This section displays the CFD results of a novel small water turbine generator for installation in a deep flow hydroponics system. The research and simulation were carried out through commercial software, namely Solidworks Flow Simulation.

1) The CFD simulation was generated using the following assumptions:
   - The water level in pipe is constant.
   - The analysis of the results determines that there is an external flow.
   - This is because some air enters the pipe at the area of the plant pot's position.
   - Rotation type is the local region (sliding).
   - Gravity is -Y direction equal to-9.81 m/s^2.

2) Parameters used in CFD analysis:
   - The periodic is equal to 0.0135 seconds (Lahamornchaiyal and Kasayapanand, 2023).
   - Setting initial conditions for substance concentrations Set the format to water and the turbulence parameters to k-epsilon.
   - The number of cores used is 8, and the installed RAM for CFD and FEA analysis in this research is 16 GB.
   - MSI Notebook Computer, Intel CORE i7, RAM 16GB.

4.3 Methods of FEA Simulation

In this study, the elasticity of PVC material is determined for developing novel small water turbine wheels, with stainless-steel materials assigned to model the shaft. Young's modulus, Poisson's ratio, shear modulus, and mass density are used to select the material characteristics of stainless steel and PVC rigidity. Table 2 displays the material qualities.

The forces caused by water speed can subsequently be applied to a novel small water turbine wheel structure. A novel small water turbine generator for installation in a deep-flow hydroponic system is analyzed under its self-weight by applying gravitational acceleration of 9.81 m/s^2 in SolidWorks Simulation software.

This study presents a static investigation into a novel small water turbine for installation in a deep-flow hydroponic system using the numerical simulation results produced and exported to simulation. A static study is performed at three different water turbine speeds: 142, 189, and 228 rpm, respectively, with selection constraints fixed at both ends of the shaft. Following that, the characteristics of the element for analysis can be adjusted to create a solid mesh, a curvature-based mesh, or Jacobian points for a high-quality mesh of 16 points. The mesh element is segmented into 130,000 according to the tetrahedron element.

Table 2
Material parameters in this research

Values	PVC rigid
Young's modulus	2,410 MPa
Poisson's ratio	0.3825
Shear modulus	866.7 MPa
Mass density	1,300 kg/m3
Values	**Stainless-steel**
Young's modulus	200,000 MPa
Poisson's ratio	0.28
Shear modulus	77,000 MPa
Mass density	7,800 kg/m^3

Source: (Solidwork, 2022; Lahamornchaiyakul and Kasayapanand, 2023)

5. Results and Discussion

The results of the CFD simulation are provided first in this study, followed by the FEA findings, which are presented and analyzed, respectively.

5.1 CFD Simulation Results

A novel small water turbine generator for installation in a water pipeline of a DFT hydroponic system was tested in the computational domain measuring 0.788x1.646x0.118m. The CFD velocity magnitude contour results obtained from using a novel small water turbine wheel rotor and water speeds between 0.0493 (6 L/min), 0.066 (8 L/min), and 0.083 m/s (10 L/min). The figure displays the type of water flow behavior that had an impact on the wheel rotor of a novel small water turbine based on the principle of CFD. As a result, clear weak flow zones and clear separate turbulent flow layers developed. Fig. 8(a) shows, the distribution of the water velocity in a water pipeline of a deep-flow hydroponics system is shown.

Turbulence kinetic energy (TKE) is the mean kinetic energy per unit mass associated with eddies in turbulent flow in fluid dynamics. The turbulent kinetic energy distribution of a water flow field at three flow rates: 6 L/min, 8 L/min, and 10 L/min. The turbulent kinetic energy distribution from the CFD is shown in Fig. 8(b), illustrating that turbulent kinetic energy occurs when the water flow makes an impact with the wheel rotor of a novel small water turbine. The results of the study reveal that, when simulating the flow field at various flow rates, it has the overall effect of reducing the turbulent kinetic energy around the vegetable-growing pot. When comparing Fig. 8(b), the turbulent kinetic energy decreased around the vegetable-growing pots. Furthermore, increasing the flow rate results in a higher Reynolds number value, etc. When considering the front of the wheel rotor, the velocity and pressure were found to be higher because the deflector had been installed. Fig. 8(c) graphically depicts the free-surface distribution of a water flow field at flow rates of 6 L/min, 8 L/min, and 10 L/min in this research. Considering the free-surface flow on the field inside the hydroponic tube, it was found to be mostly high in the surrounding area of the water turbine wheel rotor.

5.2 Calculating electrical power from a CFD simulation

The numerical simulation results show the efficiency of a set of water turbine wheel rotors capable of harvesting energy from the water flowing through the deep-flow technique hydroponic system at varying rates. According to the results of this research, the torque and mechanical power produced using a novel small

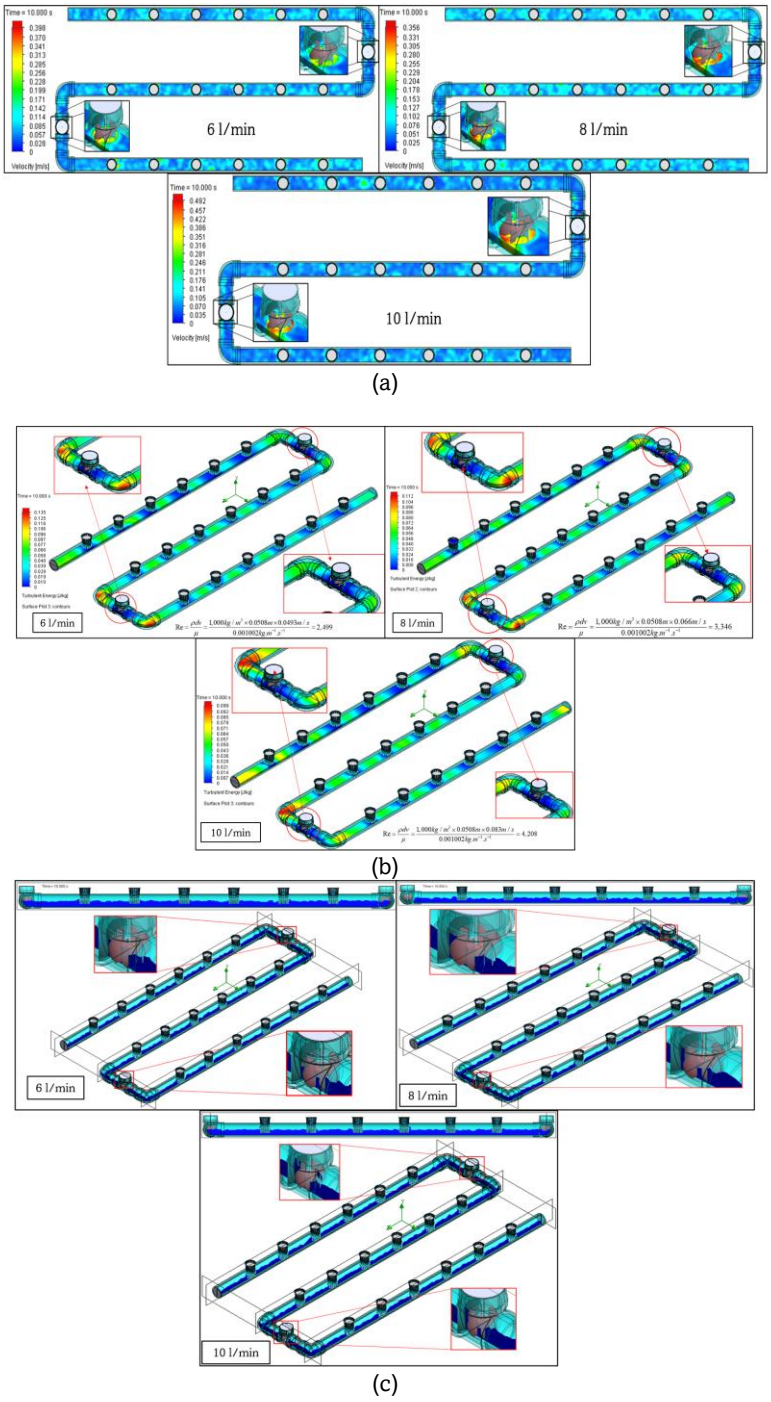

Fig. 8 depicts the numerical simulation results inside a water pipeline in a hydroponics system using a deep flow method: (a) water velocity; (b) turbulence kinetic energy; and (c) free-surface distribution of a water flow field.

water turbine generator are affected by flow rate, water speed, and rotation speed. Table 3 summarizes the empirical simulation results from this investigation. The estimated CFD parameters may then be used to create a variety of compact turbine wheel sets for even greater performance. The CFD simulation findings in this study are displayed in Fig. 8 and

Table 3
Basic document specifications

flow rate (L/min)	Volume flow rate (m^3/s)	Velocity (m/s)	Velocity of nozzle (m/s)		Speed (RPM)			Torque (N.m) (CFD)			Power (watt) (CFD)	Power (watt) (Calculation)
			Nozzle 1	Nozzle 2	Wheel 1	Wheel 2	Average	Wheel 1	Wheel 2	Average		
6	0.000102	0.0493	0.34	0.32	145	139	142	0.049	0.041	0.045	0.6687	0.4010
8	0.000134	0.0661	0.45	0.41	200	178	189	0.065	0.058	0.061	1.2065	0.6562
10	0.000167	0.0834	0.56	0.50	238	217	228	0.086	0.078	0.082	1.9568	0.8899

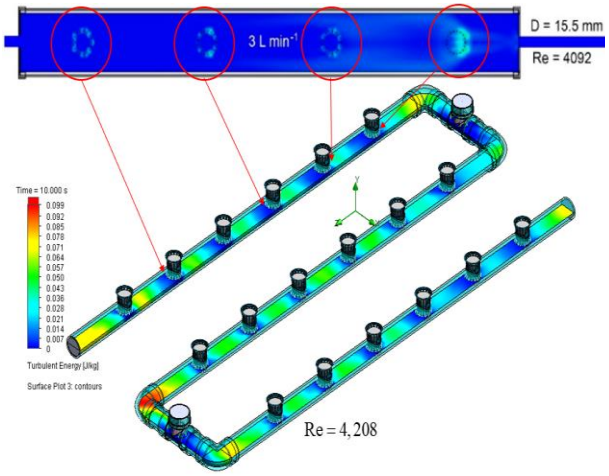

Fig. 9 depicts a comparison of the Reynolds number for a water flow field between the NFT hydroponic and deep-flow technique hydroponic systems.

Table 3. The maximum torque and power generated by a novel small water turbine generator when installed in a water pipeline of a deep-flow technique hydroponic system at a maximum flow rate of 0.000167 m^3/s (10 L/min) are 0.082 N.m. and 1.9568 watts, respectively. Similarly, when applying Equation 12, the highest mechanical power value after computing the rate of a loss throughout the pipe system is 0.8899 watts. The specific type of water turbine employed influences the conversion efficiency of a hydroelectric power plant, which may be as high as 90–95% for large installations (Woodbank Communications Ltd., 2005; Marco, 2015; Lahamornchaiyakul and Kasayapanand, 2023). The novel small water turbine in this research obtained 80% performance efficiency as a design guideline.

5.3 FEA Simulation Results

SolidWorks Flow Simulation software can be used to analyze the water flow field under the rotation of the water turbine wheel in various conditions and present the results of such analysis. Continuing with the calculations in static analysis, data can be exported through an option called "Export Result to Simulation.". The FEA simulation results are shown in Fig. 10.

The results obtained from this research, when taken into consideration and compared with the research of Guzman-Valdivia et al. (Guzman-Valdivia *et al.,* 2019), who studied water flow using the NFT hydroponic system, indicate that Reynolds numbers in the range of 4,000–4,200 flowing through NFT hydroponic systems and deep-flow hydroponic systems were similar in the area around the vegetable pots, with subsequent variations in values. The comparison can be seen in Fig. 9.

In this study, an investigation of the Von Misses stress and displacement was done on a range of rotational speeds for the water turbine blades. Table 3 shows the results of a water turbine wheel revolving at 142, 189, and 228 rpm. The results are summarized in Table 4.

It shows the employment of different forces on the wheel speed to find the structure's maximum strength for a novel small water turbine generator for installation in a deep-flow hydroponic system. The maximum von Mises stresses at a wheel speed of 228 rpm for a novel small water turbine generator for installation in a deep-flow hydroponic system are 2.4x10-3 MPa, as shown in Fig. 10(c). The total deformation when the water jet impacts the wheel structure of a novel small water turbine generator is maximum at the blade of the structure. The maximum value of the total deformation at a wheel speed of 228 rpm is 7.0 x 10^{-5} mm, as shown in Fig. 10 (c). The wheel of a new water turbine generator's wheel had a maximum rotation speed of 228 rpm, a maximum safety factor of 10 ul, and a minimum of 1.25 ul. The safety factor values found in this study can be used to optimize the design.

Considering the rotation speed at 228 rpm, the maximum value obtained from the analysis in Table 4 shows significantly similar values. The Von-Misses stress values affecting displacements at different rotational speeds are mainly formed in the direction of the Z-axis. When comparing the numerical simulation results in NFT hydroponic systems between Cesar et al. and the novel small water turbine generator for installation in a water pipeline on a deep-flow technique hydroponics system, the flow field difference was found to be 2.84%.

The numerical results obtained by CFD and FEA simulations led to the further development of prototypes for a novel small water turbine generator for installation in a deep-flow hydroponic system to produce electricity. Based on the results of the study, this type of novel small water turbine can be applied to any closed-flow, deep-flow hydroponic system.

6. Conclusions

This research focuses on the design and investigation of a novel small water turbine generator for installation in a deep-flow hydroponic system. Based on the findings, it can be inferred that a novel small water turbine generator is suitable for use in water pipelines and deep-flow hydroponic systems. For water flow rates, the mechanical efficiency is indicated to be 80%. Furthermore, the real outcomes of the study are based on theoretical and experimental fluid simulations. After identifying the available parameters, the fundamentals of building and analyzing the mechanical elements of a novel water turbine generator for installation in a deep-flow hydroponic system are based on the general principles of a water turbine design. The completion of FEA numerical simulations can enable the calculation of von Mises stress results and deformations. CFD simulation computes the outcomes of rotational speeds and the amount of power that water turbines can finally produce. The mechanical efficiency of a novel small water turbine generator designed and developed for installation in a deep-flow hydroponic system is about 80% (Lahamornchaiyakul and Kasayapanand, 2023), which is quite good and should be used as a guideline for the initial design. The computation of variables resulting from mathematical equations and numerical

Table 4
FEA simulation results of a novel small water turbine generator for installation in a deep-flow hydroponic system

Results	Wheel speed					
	142 rpm		189 rpm		228 rpm	
	Max	Min	Max	Min	Max	Min
Von misses stress (MPa)	$9.5x10^{-4}$	$1.0x10^{-4}$	$1.7x10^{-3}$	$2.0x10^{-4}$	$2.4x10^{-3}$	$2.0x10^{-4}$
Displacement (mm.)	$2.5x10^{-5}$	$3.0x10^{-6}$	$4.5x10^{-5}$	$4.0x10^{-6}$	$7.0x10^{-5}$	$1.0x10^{-5}$

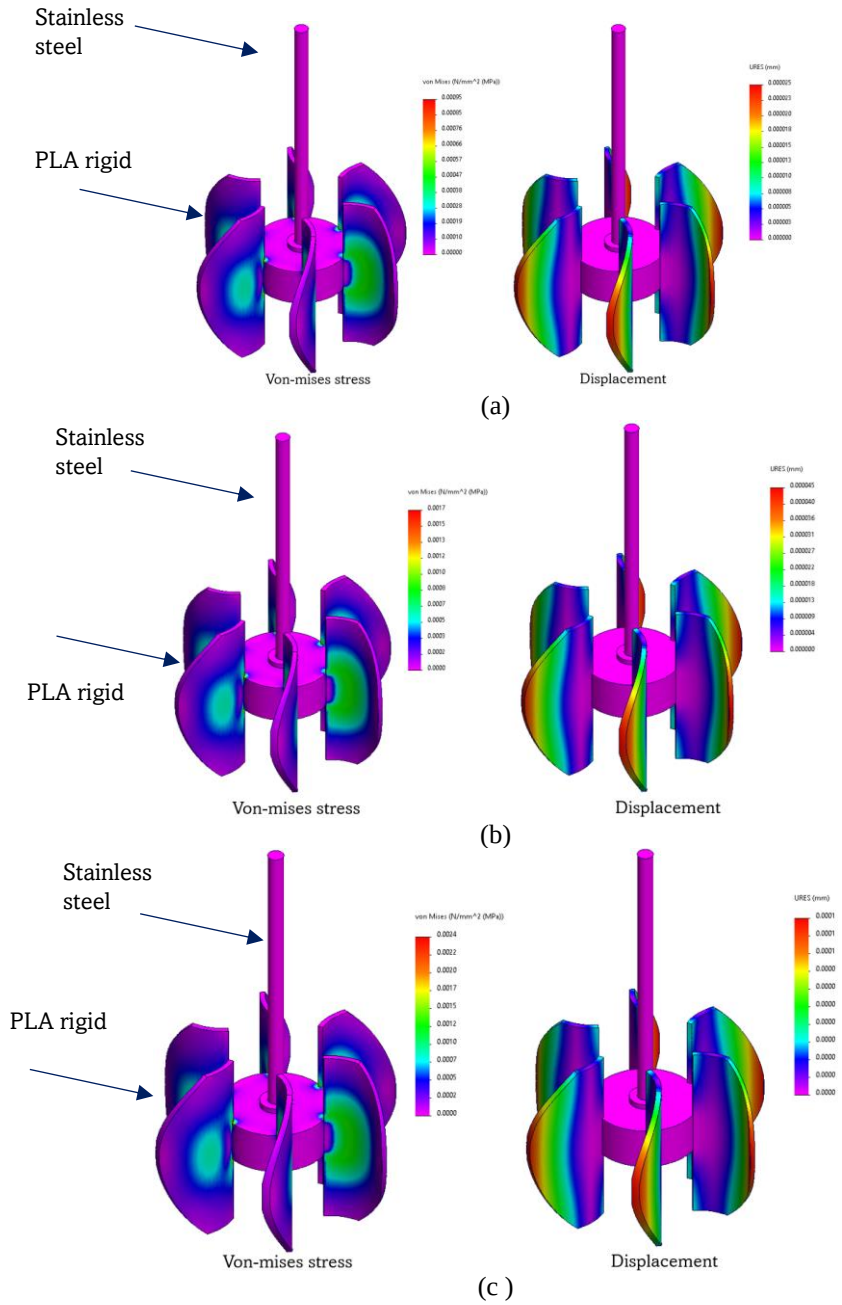

Fig. 10 depicts 3D Von-Misses stress and displacement at (a) 142rpm, (b) 189 rpm, (c) 228 rpm

simulation appears to be the optimum combination for building an efficient and novel small water turbine generator for installation in a deep-flow hydroponic system. Furthermore, effective implementation will reduce Thailand's need for electricity while requiring little in the way of maintenance and installation costs.

Acknowledgments

The Department of Mechanical Engineering, Faculty of Engineering, Rajamangala University of Technology, Lanna, Thailand, provided financial assistance for this study and has provided support for various calculation equipment and software until this research was successfully completed.

References

Abdulah, M. and Muhammed, S.D. (2022). Modeling spherical turbine for in-pipe energy conservation. *Ocean Engineering*, 246(2022),110497; https://doi.org/10.1016/j.oceaneng.2021.110497

Autodesk Simulation CFD, Autodesk Simulation CFD, Produced by Autodesk Inc., 2015, http:// www.autodesk.com/cfd. Accessed on 3 November 2022

Baiyin, B., Tagawa, K., Yamada, M., Wang, X., Yamada, S., Shao, Y., An, P., Yamamoto, S., & Ibaraki, Y. (2021). Effect of Nutrient Solution Flow Rate on Hydroponic Plant Growth and Root Morphology. *Plants* (MDPI), 10, 1840; https://doi.org/10.3390/plants10091840

Baris. (2021) *plant 28*. https://grabcad.com/library/plant-28-1. Accessed on 12 May 2023.

Chen, H., Kan, K., Wang, H., Binama, M. and Xu, H. (2021). Development and Numerical Performance Analysis of a Micro Turbine in a Tap-Water Pipeline. *Sustainability,* 13(19), 10755; https://doi.org/10.3390/su131910755

Chen, J., Hongxing, Y., Liu, C.P., Lau, C. H. and Lo, M. (2013). A novel vertical axis water turbine for power generation from water pipelines. *Energy,* 54(2013), 184-193; https://doi.org/10.1016/j.energy.2013.01.064

Dmitriev, S., Kurkin, A., Dobrov, A., Doronkov, D., Pronin, A., & Solntsev, D. (2023). CFD Modeling of Heat Exchanger with Small Bent Radius Coils Using Porous Media Model. *Fluid* (MDPI), 8, 141; https://doi.org/10.3390/fluids8050141

EL-Sayed I.I.M. and Ahmed Farouk A.R., (2019). In-Pipe Micro-Hydropower Systems for Energy Harvesting. In 4th IUGRC International Undergraduate Research Conference. https://www.academia.edu/39999108/In_Pipe_Micro_Hydrop

Ebhota, W.S. and Inambao, F.L (2015). Domestic Turbine Design, Simulation and Manufacturing for Sub-Saharan Africa Energy Sustainability. *In the 14th International Conference on Sustainable Energy Technologies-SET* 2015. https://www.academia.edu/30931929/Domestic_Turbine_Design_Simulation_and_Manufacturing_for_SubSaharan_Africa_Energy_Sustainability

Guzman-Valdivia, C.H., Talavera-Otero, J., & Desiga-Orenday, O. (2019). Turbulent Kinetic Energy Distribution of Nutrient Solution Flow in NFT Hydroponic Systems Using Computational Fluid Dynamics. *AgriEngineering*, 2019(1), 289-290; https://doi:10.3390/agriengineering1020021

Gandhi, O., Ramdhani, M., Ary Murti, M., & Setianingsih, C. (2019). Water Flow Control System Based on Context Aware Algorithm and IoT for Hydroponic. *2019 IEEE International Conference on Internet of Things and Intelligence System (IoTaIS),* 212-217; https://doi:10.1109/IoTaIS47347.2019.8980373

Ghada, D., Mohamed, E. and Ahmed, M.A.S. (2022). Performance Assessment of Lift-Based Turbine for Small-Scale Power Generation in Water Pipelines using OpenFOAM. *Engineering Applications of Computational Fluid Mechanics*, 16(1), 536-550; https://doi.org/10.1080/19942060.2021.2019129

Hasanzadeh, N., Payambarpour, S. A., Najafi, A. F., & Magagnato, F. (2021). Investigation of in-pipe drag-based turbine for distributed hydropower harvesting: Modeling and optimization. *Journal of Cleaner Production*, 298, 126710; https://doi.org/10.1016/j.jclepro.2021.126710

Hosain, A., Morteza, K. and Jaber, S. (2020). Experimental investigation and numerical simulation of an inline low-head microhydroturbine for applications in water pipelines. *IET Renewable Power Generation,* 14(16), 3209-3219; https://doi.org/10.1049/iet-rpg.2019.1283

Jiyun, D., Hongxing, Y., Zhicheng, S., & Xiaodong, G. (2018). Development of an inline vertical cross-flow turbine for hydropower harvesting in urban water supply pipes. *Renewable, Energy*, 127, 386–397; https://doi.org/10.1016/j.renene.2018.04.070

Jaruwongwittaya, T., Boonjue, A., Amattirat, N., Suttiprapa, P., Vengsungnle, P., & Nuboon, T. (2015). Investigation of the length and the number of gutter optimal for chilled water circulation in hydroponics planting. *Frame Engineering and Automation Technology Journal*, 1(2), 67-74; https://ph02.tci-thaijo.org/index.php/featkku/article/view/176149/125753

Kumkuang, S. (2017). The Design and Fabrication of Economy Nutrient Flow Technique Vegetable Hydroponics Set. *CRMA Journal*, 15(2017), 91-99; https://ph01.tci-thaijo.org/index.php/crma-journal/article/view/243106/165336

Lahamornchaiyakul, W., & Kasayapanand, N. (2023). The Design and Analysis of a Novel Vertical Axis Small Water Turbine Generator for Installation in Drainage Lines. *International Journal of Renewable Energy Development*, 12(2), 235-246; https://doi.org/10.14710/ijred.2023.48388

Lahamornchaiyakul, W., & Kasayapanand, N. (2023). Free-Spinning Numerical Simulation of a Novel Vertical Axis Small Water Turbine Generator for Installation in a Water Pipeline. *CFD Letters*, 15(8), 31-49; https://doi.org/10.37934/cfdl.15.8.3149

Lahamornchaiyakul, W. (2021). The CFD-Based Simulation of a Horizontal Axis Micro Water Turbine, *Walailak Journal of Science and Technology,* 18(7), 9238; https://doi.org/10.48048/wjst.2021.9238

Lahamornchaiyakul, W. (2023). FEA-Based Simulation of a Small Water Turbine for Waterfall, science and technology asia. *Science & Technology Asia,* 28(1), 152-168; https://doi.org/10.14456/scitechasia.2023.13

MR CFD Company, *what is Multiple Reference Frames (MRF).*, 2023, https://www.mr-cfd.com/services/fluent-modules/moving-reference-frame. Accessed on 16 October 2023.

Ma, T., Yang, H., Guo, X., Lou, C., Shen, Z., Chen, J., & Du, J. (2018). Development of inline hydroelectric generation system from municipal water pipelines. *Energy,* 144, 535–548; https://doi.org/10.1016/j.energy.2017.11.113

Muhammad, H.T., Shoukat, A.M., Salman, A., Mughees, S., Nouman, Z., Muhammad, A.M., Arsalan, M. and Muhammad, A.S. (2020). Production of electricity employing sewerage lines using a micro cross flow turbine. *International Journal of Engineering, Science and Technology,* 12(2), 67-77; https://doi.org/10.4314/ijest.v12i2.8

Mosbahi, M., Ayadi, A., Mabrouki, I., Driss, Z., Tucciarelli, T., Abid, M.S. (2019). Effect of the Converging Pipe on the Performance of a Lucid Spherical Rotor. *Arab. J. Sci. Eng,* 44, 1583–1600; https://doi.org/10.1007/s13369 018 3625 0

McLean, D. (Eds.) (2012). Understanding Aerodynamics. John Wiley & Sons, Ltd. Chichester, UK.

Muhammad, S.A., Muhammad, A.K., Harun, J., Faisal, J., Alexander, C. and Kim, D.O. (2021). Design and Analysis of In-Pipe Hydro-Turbine for an Optimized Nearly Zero Energy Building. *Sensors,* 21(23), 8154; https://doi.org/10.3390/s21238154

Muhammad, H.T., Shoukat, A.M., Salman, A., Mughees, S., Nouman, Z., Muhammad, A.M., Arsalan, M. and Muhammad, A.S. (2020). Production of electricity employing sewerage lines using a micro cross flow turbine. *International Journal of Engineering, Science and Technology,* 12(2), 67-77; https://doi.org/10.4314/ijest.v12i2.8

Marco, C. (2015). Harvesting energy from in-pipe hydro systems at urban and building scale. *International Journal of Smart Grid and Clean Energy,* 4(4), 316-327; https://doi.org/10.12720/sgce.4.4.316-327

Nasir, B.A. (2013). Design of High Efficiency Cross-Flow Turbine for Hydro-Power Plant. *International Journal of Engineering and Advanced Technology*, 2(3), 308-311. https: https://www.ijeat.org/wpcontent/uploads/papers/v2i3/C1115022313.pdf

Niam, A.G., Suhardiyant, H., Seminar, B.O., & Madd, A. (2017). CFD Simulation of Cooling Pipes Distance in The Growing Medium for Hydroponic Substrate in Tropical Lowland. *International Journal of Engineering Research and Development*, 15(1), 56-63; http://ijerd.com/paper/vol13-issue1/Version-1/I1315663.pdf

Oladosu, T.L. and Koya, O.A. (2018). Numerical analysis of lift-based in-pipe turbine for predicting hydropower harnessing potential in selected water distribution networks for waterlines optimization. *Engineering Science and Technology, an International Journal*, 21(4), 672-678; https://doi.org/10.1016/j.jestch.2018.05.016

Phaengkieo, D., Chaoumead, A., Wangngon, B., & Chumnumwat, S. (2019). The application of nanobubble technology for DRFT hydroponics. *Journal of Innovative Technology Research*, 3(2), 33-41; https://so04.tci-thaijo.org/index.php/JIT/article/view/242537/164799

Patel, A., & Dhakar, P.S. (2018). CFD Analysis of Air Conditioning in Room Using Ansys Fluent. *Journal of Emerging Technologies and Innovative Research (JETIR)*, 5(11), 436-441; https://doi:10.13140/RG.2.2.13462.50249

Patel, M. and Oza, N. (2016). Design and Analysis of High Efficiency Cross-Flow Turbine for Hydro-Power Plant. *International Journal of Engineering and Advanced Technology*, 5(4), 187-193. https://www.ijeat.org/wp-content/uploads/papers/v2i3/C1115022313.pdf

Solidworks, *Solidworks Simulation, Solidworks Flow Simulation, Produced by Solidworks Corporation*., 2022, https://www.solidworks.com. Accessed on 12 October 2022.

Thabet, S., & Thabit, T.H. (2018). CFD Simulation of the Air Flow around a Car Model (Ahmed Body). *International Journal of Scientific and*

Research Publications, 8(7), 517-524; https://doi:10.29322/IJSRP.8.7.2018.p7979

Vega, I., Bien-Amie, D., Augustin, G., Heiden, W., & Heiden, N. (2023). Intermittent circulation of simplified deep flow technique hydroponic system increases yield efficiency and allows application of systems without electricity in Haiti. *Agriculture & Food Security,* 12(18), 1-9; https://doi.org/10.1186/s40066-023-00422-8

Vaishaly, P. and Romarao, S. (2015). Finite element stress analysis of a typical stream turbine blade. *International Journal of Science and Research (IJSR),* 4(7), 1059-1065. https://www.ijsr.net/archive/v4i7/SUB156518.pdf

Wang, C.N., Yang, F.C., Nguyen, V.T.T., & Vo, N.T.M. (2022). CFD Analysis and Optimum Design for a Centrifugal Pump Using an Effectively Artificial Intelligent Algorithm. *Micromachines (MDPI)*, 13, 1208; https://doi.org/10.3390/mi13081208

Woodbank Communications Ltd, (2005). Hydroelectric Power. Retrieved 12 October 2022, from https://www.mpoweruk.com/hydro_power.htm.

Yeo, H., Seok, W., Shin, S., Huh, Y.C., Jung, B.C., Myung, C.S. and Rhee, S.H. (2019). Computational Analysis of the Performance of a Vertical Axis Turbine in a Water Pipe. *Energies*, 12(20), 3998; https://doi.org/10.3390/en12203998

Zhuohuan, H.U., Dongcheng, W., Wei, L.U., Jian, C. and Yuwen, Z. (2020). Performance of vertical axis water turbine with eye-shaped baffle for pico hydropower. *Front. Energy*, 1-4; https://doi.org/10.1007/s11708-020-0689-9

3Dponics. (2015). *Planter - 3Dponics Cube System*. https://grabcad.com/library/planter-3dponics-cube-system-1. Accessed on 12 May 2023